Vol 13 No 1, January 2004
1009-1963/2004/13(01)/0047-07

Chinese Physics

© 2004 Chin. Phys. Soc.
and IOP Publishing Ltd

Lattice Boltzmann method for three-dimensional moving particles in a Newtonian fluid*

Fang Hai-Ping(方海平)[a)b)†] and Chen Shi-Yi[b)]

[a)] *Shanghai Institute of Nuclear Research, Chinese Academy of Sciences, Shanghai* 201800, *China*

[b)] *Department of Mechanical Engineering, the Johns Hopkins University, MD* 21218, *USA*

(Received 23 May 2003; revised manuscript received 1 September 2003)

A lattice Boltzmann method is developed to simulate three-dimensional solid particle motions in fluids. In the present model, a uniform grid is used and the exact spatial location of the physical boundary of the suspended particles is determined using an interpolation scheme. The numerical accuracy and efficiency of the proposed lattice Boltzmann method is demonstrated by simulating the sedimentation of a single sphere in a square cylinder. Highly accurate simulation results can be achieved with few meshes, compared with the previous lattice Boltzmann methods. The present method is expected to find applications on the flow systems with moving boundaries, such as the blood flow in distensible vessels, the particle–flow interaction and the solidification of alloys.

Keywords: lattice Boltzmann method, suspension, Newtonian fluid
PACC: 4755

1. Introduction

In the past decade, the lattice Boltzmann method (LBM) [1−3] has been proved competitive in studying the domain of fluid flow for various physical systems. The method is based on the discrete Boltzmann equation and inherits the advantage of local nature of the computation. The lattice Boltzmann method has been proved to achieve second-order accuracy in the domain of the fluid both theoretically and numerically.[4] The application of the lattice Boltzmann method to study the solid particle in fluid was first considered by Ladd.[5] In Ref.[5], Ladd proposed a modified bounce-back rule to meet the non-slip boundary condition at moving boundaries and a scheme based on momentum-exchange to calculate the hydrodynamic force exerting on the solid particles. Aidun *et al*[6] tried to improve Ladd's model by removing the fluid within the solid region so that they could handle a solid with a density less than that of the fluid. Behrend[7] analysed the different boundary conditions based on the bounce-back rule and proposed a "related bounce back at the nodes"(RBBN). Both Ladd's and Aidun's models assumed the physical boundary located in the middle of the link between a solid node and a fluid node. Consequently, the hydrodynamic force would exert on the middle of the link. The exact location of the physical boundary for the Behrend model is more difficult to determine. Consequently, it is possible that the hydrodynamic radius of a suspended particle differs from the input radius for these three models.[8] Recently, Noble and Torczynski[9] proposed a lattice Boltzmann model to study the system in which computational cells are partially filled with fluid. Fang *et al*[10,11] applied the lattice Boltzmann method to the study of the fluid flow in distensible blood vessels. Inamuro *et al*[12] studies the neutrally buoyant circular cylinders in the flow between parallel walls.

In order to obtain a high-order accuracy lattice Boltzmann model, the exact spatial location of the physical boundary is important. Any change of the location of the physical boundary should be taken into account in the boundary condition and the hydrodynamic force exerted on the moving boundary. Recently, Filippova and Hanel[13] presented a boundary condition for the stationary complex geometry. The parameters for the scheme depend on the exact location of the physical boundary explicitly. The stability and robustness have been proved and improved by

*Project supported in part by the National Natural Science Foundation of China (Grant No 19904004).
†E-mail: hpfang2000@yahoo.com

Mei *et al.*[14,15] In our previous paper, we proposed a two-dimensional (2D) lattice Boltzmann scheme to simulate solid particle motions in fluids.[16] The numerical accuracy of the proposed scheme is demonstrated by simulating the sedimentation of a circular cylinder in a 2D channel. Excellent agreement is shown between the lattice Boltzmann method and a second-order moving finite-element method;[17,18] and a nearly second-order spatial convergence demonstrates that the proposed lattice Boltzmann method is an effective and efficient direct numerical simulation (DNS) method for simulating particle motions in fluids in two dimensions. In this paper, the proposed lattice Boltzmann scheme is extended and implemented for a three-dimensional (3D) scheme. The 3D simulation results on a single sphere in a square tube at very low Reynolds numbers with few meshes agree with experimental data to a high accuracy. The time-dependent behaviour of a circular cylinder in a 2D channel from simulations coincides with the previous 2D scheme very well.

This paper is organized as follows. In Section 2 we briefly describe the 3D lattice Boltzmann method. Section 3 is devoted to a review of the boundary condition for complex geometry proposed by Filippova and Hanel. In Section 4, the distribution functions on the new-born fluid node due to the moving particles and the hydrodynamics force exerted on them are considered. We present our simulation results on Section 5. Conclusions and discussion are presented in Section 6.

2. The lattice Boltzmann model

Let $f_i(\boldsymbol{x},t)$ be a non-negative real number describing the distribution function of the fluid density at site $\boldsymbol{x}$ at time t moving in direction $\boldsymbol{e}_i$. In the model Q15D3 on a 3D cubic lattice, there are 15 discrete velocities

$$\boldsymbol{e}_i = \begin{cases} (0,0,0), & i=0; \text{rest particle}, \\ (\pm1,0,0)c, (0,\pm1,0)c, (0,0,\pm1)c, & i=1,2,\cdots,6, \\ (\pm1,\pm1,\pm1)c, & i=7,8,\cdots,14. \end{cases}$$

The distribution functions evolve according to a Boltzmann equation that is discrete in both space and time:[2,3]

$$f_i(\boldsymbol{x}+\boldsymbol{e}_i, t+1) - f_i(\boldsymbol{x},t) = -\frac{1}{\tau}(f_i - f_i^{\rm eq}). \quad (1)$$

The equilibrium distribution functions $f_i^{\rm eq}$ are usually supposed to be dependent only on the local density ρ and flow velocity $\boldsymbol{u}$

$$f_i^{\rm eq} = \alpha_i \rho \left[1 + \frac{3}{c^2}\boldsymbol{e}_i\cdot\boldsymbol{u} + \frac{9}{2c^4}(\boldsymbol{e}_i\cdot\boldsymbol{u})^2 - \frac{3}{2c^2}u^2\right], \quad (2)$$

with

$$\alpha_i = \begin{cases} 2/9, & i=0; \text{rest particle}, \\ 1/9, & i=1,2,\cdots,6, \\ 1/72, & i=7,8,\cdots,14, \end{cases}$$

and ρ and $\boldsymbol{u}$ are defined as

$$\rho = \sum_i f_i, \quad \rho\boldsymbol{u} = \sum_i f_i \boldsymbol{e}_i. \quad (3)$$

The macroscopic equations can be obtained by a Chapman–Enskog procedure. They are the continuity equation

$$\partial_t \rho + \partial_\alpha(\rho u_\alpha) = 0, \quad (4)$$

and the Navier–Stokes equations

$$\begin{aligned} &\partial_t(\rho u_\alpha) + \partial_\beta(\rho u_\alpha u_\beta) \\ =&\partial_\alpha p + \nu\partial_\beta[\rho(\partial_\alpha u_\beta + \partial_\beta u_\alpha)], \end{aligned} \quad (5)$$

where ν is the viscosity, defined by the equation

$$\nu = \frac{(2\tau-1)}{6}c^2\delta t. \quad (6)$$

In this paper, we set $\delta x = \delta t = c = 1$.

3. Boundary condition for complex geometry

Filippova and Hanel [13] presented their scheme for treating the boundary condition by considering a curved boundary lying between the equidistant lattice nodes of space δx as shown in Fig.1 for a 2D projection of a 3D body. The lattice nodes on the solid and fluid sides are denoted by $\boldsymbol{x}_b$ and $\boldsymbol{x}_f$ respectively. We assume

$$\boldsymbol{e}_i = \boldsymbol{x}_b - \boldsymbol{x}_f,$$

and

$$\boldsymbol{e}_{\bar{i}} = -\boldsymbol{e}_i.$$

The small solid circle at $\boldsymbol{x}_w$ is the intersection of the link between $\boldsymbol{x}_b$ and $\boldsymbol{x}_f$ with the physical boundary. The fraction of an intersected link in the fluid is Δ:

$$\Delta = \frac{|\boldsymbol{x}_f - \boldsymbol{x}_w|}{|\boldsymbol{x}_f - \boldsymbol{x}_b|}, \quad 0 \le \Delta \le 1. \quad (7)$$

After the collision step, at time t, the distribution functions at $\boldsymbol{x}_f$ are known. In the streaming step $f_{\bar{i}}(\boldsymbol{x}_f)$ is expected to be obtained by

$$f_{\bar{i}}(\boldsymbol{x}_f, t+\delta t) = f_{\bar{i}}(\boldsymbol{x}_b, t). \tag{8}$$

However, the distribution function $f_{\bar{i}}(\boldsymbol{x}_b, t)$ at the boundary node is unknown.

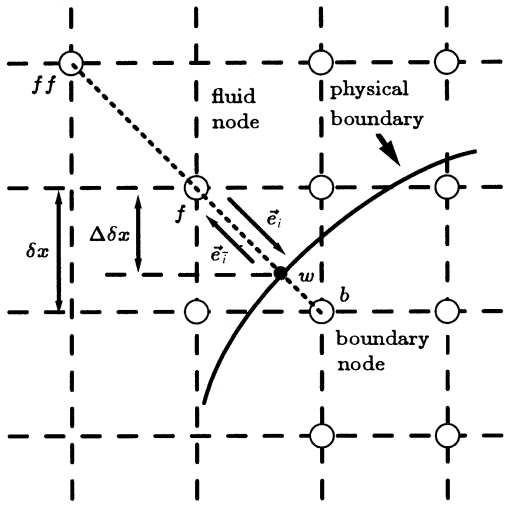


Fig.1. A 2D projection of the layout of the regularly spaced lattices and curved wall boundary.

Filippova and Hanel assumed a linear interpolation [13]

$$\begin{aligned} f_{\bar{i}}(\boldsymbol{x}_b, t) =& (1-\chi) f_i(\boldsymbol{x}_f, t) \\ &+ \chi f_i^{(*)}(\boldsymbol{x}_b, t)(\boldsymbol{x}_b, t) + 6\alpha_i \boldsymbol{e}_{\bar{i}} \cdot \boldsymbol{u}_w, \end{aligned} \tag{9}$$

where $\boldsymbol{u}_w = \boldsymbol{u}(\boldsymbol{x}_w, t)$ is the velocity at $\boldsymbol{x}_w$, and χ is a parameter. $f_i^{(*)}$ is a fictitious equilibrium distribution function given by

$$f_i^{(*)}(\boldsymbol{x}_b, t) = \alpha_i \rho \left[1 + 3\boldsymbol{e}_i \cdot \boldsymbol{u}_{bf} + \frac{9}{2}(\boldsymbol{e}_i \cdot \boldsymbol{u}_f)^2 - \frac{3}{2} u_f^2 \right], \tag{10}$$

where $\boldsymbol{u}_f = \boldsymbol{u}(\boldsymbol{x}_b, t)$ is the fluid velocity at the fluid node f, as shown in Fig.1; $\boldsymbol{u}_{bf}$ is to be determined below. Fillippova and Hanel proposed

$$\begin{aligned} &\boldsymbol{u}_{bf} = (\Delta - 1)\boldsymbol{u}_f/\Delta + \boldsymbol{u}_w/\Delta, \\ &\chi = (2\Delta - 1)/\tau \quad \text{for} \quad \Delta \geq \frac{1}{2}, \end{aligned} \tag{11}$$

and

$$\boldsymbol{u}_{bf} = \boldsymbol{u}_f \quad \text{and} \quad \chi = (2\Delta - 1)/(\tau - 1) \quad \text{for} \quad \Delta \leq \frac{1}{2}, \tag{12}$$

to obtain a second-order scheme for the "slow flow". Mei *et al*[14] improved the stability of the scheme by replacing Eq.(12) by

$$\boldsymbol{u}_{bf} = \boldsymbol{u}_{ff} \quad \text{and} \quad \chi = (2\Delta - 1)/(\tau - 2) \quad \text{for} \quad \Delta \leq \frac{1}{2}. \tag{13}$$

They have used the improved technique to test several flow problems, such as the fully developed flow in a square duct, the 3D lid-driven cavity flows, fully developed flows inside a circular pipe and a uniform flow over a sphere to demonstrate its accuracy and robustness.[15]

4. Boundary condition for moving boundaries and hydrodynamic force on a solid particle

When a fluid node is covered by a moving solid particle, the fluid at this node will removed from the system. On the other hand, when a fluid node previously occupied by a solid particle is recovered, the fluid density at this newly created node is assumed to be the average of the extrapolated values from a second-order extrapolation scheme of all the possible directions.[16]

For each relevant direction $\boldsymbol{e}_{\bar{i}}$ from a fluid node to a boundary node, the solid boundary obtains an amount of moment $[f_i(\boldsymbol{x}_f, t_+) + f_i(\boldsymbol{x}_f, t_+)]\boldsymbol{e}_i$ by a fraction of particles $f_i(\boldsymbol{x}_f, t_+)$ acted on it along the direction $\boldsymbol{e}_i$ and pushing a fraction of particles $f_{\bar{i}}(\boldsymbol{x}_b, t)$ into fluid along the direction $-\boldsymbol{e}_i$ in a time step. Consequently, the hydrodynamic force exerted on the solid particle at time t along this direction is

$$\boldsymbol{F}(\boldsymbol{x}_b) = [f_{\bar{i}}(\boldsymbol{x}_b, t) + f_i(\boldsymbol{x}_f, t_+)]\boldsymbol{e}_i, \tag{14}$$

where t_+ is the post-collision time, and $f_{\bar{i}}(\boldsymbol{x}_b, t)$ is obtained from Eq.(9). The total force $\boldsymbol{F}_{\mathrm{T}}$ and torque $\boldsymbol{T}_{\mathrm{T}}$ acting on the solid particle are

$$\boldsymbol{F}_{\mathrm{T}} = \sum \boldsymbol{F}(\boldsymbol{x}_b), \tag{15}$$

and

$$\boldsymbol{T}_{\mathrm{T}} = \sum (\boldsymbol{x}_b - \boldsymbol{R}) \times \boldsymbol{F}(\boldsymbol{x}_b), \tag{16}$$

where $\boldsymbol{R}$ is the centre of mass of the solid particle. The summation runs over all the relevant directions.

The translations of the centre of mass of each particle are updated at each Newtonian dynamic time step by using a so-called half-step 'leap-frog' scheme.[19]

5. Simulation and results

5.1. Wall correction factor of single solid spheres in a square cylinder

Particles moving in a narrow space are influenced by the wall. In 1981, Miyamura *et al*[20] set up experiments to study the wall effect to obtain the wall correction factor. We will demonstrate the accuracy and efficiency of the present scheme by simulating a spherical particle in a vertical square channel and comparing with the experiment. The sphere is initially released at the centre of the cross-section of the channel with zero velocity. The diameter of the particle is d and the width of the channel is L. Due to the wall effect the terminal velocity of the particle will be less than the terminal velocity of an unconfined particle. The lattice Boltzmann simulation has been carried out for the 3D sedimentation in the same conditions as for the experiment. In the present analysis, the channel is divided into $512 \times 32 \times 32$ lattice units. Both the inlet and outlet (downstream boundary) of the domain are always larger than 250 lattice units from the moving particles. Zero velocities are applied uniformly to the inlet and the normal derivative of the velocity is set to zero at the outlet. The terminal particle Reynolds number, defined as $Re = du_{\rm p}/\nu$, where $u_{\rm p}$ is the terminal velocity of the particle. In the present simulations, Re is about 0.01. This Reynolds number is small enough to use the Stokes equation to calculate the terminal velocity u_0 of a spherical particle in unconfined space.

The wall correction factor is defined as

$$\eta = u_{\rm p}/u_0.$$

Figure 2 shows the simulation results together with the best curve fit to the experimental data of Miyamura *et al*.[20] Excellent agreement between the experimental data and our simulation results can be clearly seen. In this figure, we also show the computational results by Aidun *et al*[6] in which the channel is divided into $512 \times 32 \times 32$ lattice units and $1024 \times 64 \times 64$ lattice units. Since the exact spatial location of the physical boundary of the suspended particles is determined in the present scheme, we can reach a high accuracy with few meshes. We emphasize that although only $512 \times 32 \times 32$ meshes are used in the present simulations, the consistence with experiment is better than those by Aidun *et al*[6] with $1024 \times 64 \times 64$ meshes.

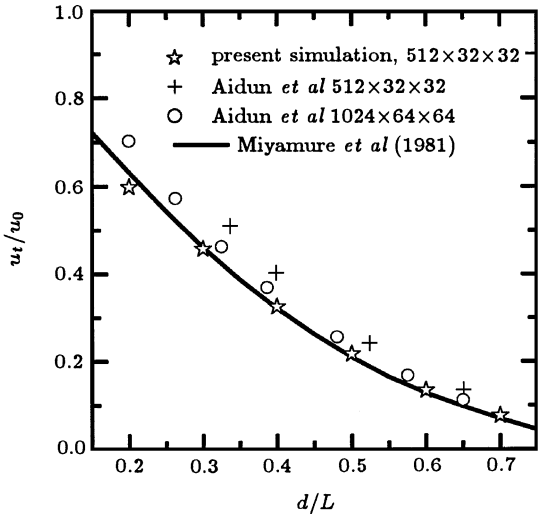


Fig.2. Wall effect of a single sphere settling in a long square tube. The solid line is a best fit to the experimental data of Miyamura *et al*.[20] The stars are the present lattice Boltzmann simulations while the data points ◯ and + are taken from the computational analysis of Aidun *et al*.[6]

5.2. Sedimentation of a circular cylinder in a 2D channel

In our previous paper, we studied the behaviour of a circular cylinder driven by gravity in a vertical channel. Our 2D simulation results agree with those using a finite-element method.[17,18] In this section, we will show the detailed comparison between the 2D and 3D lattice Boltzmann simulation results. The system is a vertical channel of width L. $L = 4d$, where d=0.1cm is the diameter of the cylinder. The y-axis is vertically downward on the left wall. The cylinder is released at x=0.075cm and then settles under gravity. The density and the kinematic viscosity of the fluid flow are 1g/cm^3 and 0.01cm^2/s. In our simulation, the inlet of the domain is always $10d$ from the moving particles, whereas the downstream boundary is $15d$ from the boundary. Zero velocities are applied uniformly to the inlet and the normal derivative of the velocity is set to zero at the outlet.

In the 2D lattice Boltzmann simulation, the radius of the cylinder is 13 lattice units; τ=0.6. The solid densities in the simulation are 1.0015, 1.003, 1.01 and 1.03g/cm^3 respectively.

This system can also be simulated in 3D lattice Boltzmann method by considering the full 3D circular cylinder. Explicitly, the width in the z-direction is four lattice units and the periodic boundary condition is applied in the z-direction. The radius of the cylinder is seven lattice units in the simulation. All the other settings are the same as those in the 2D case.

Figure 3 displays the trajectories of the cylinder. Excellent consistence can be observed. The agreement between our 2D and 3D lattice Boltzmann simulations can be seen more prominently by examining the angular velocity for different terminal Reynolds number which are shown in Fig.4. These simulations results show that the three-dimensional lattice Boltzmann scheme presented in the present paper is a good extension of the 2D method [16] and further demonstrate the accuracy of the present 3D method.

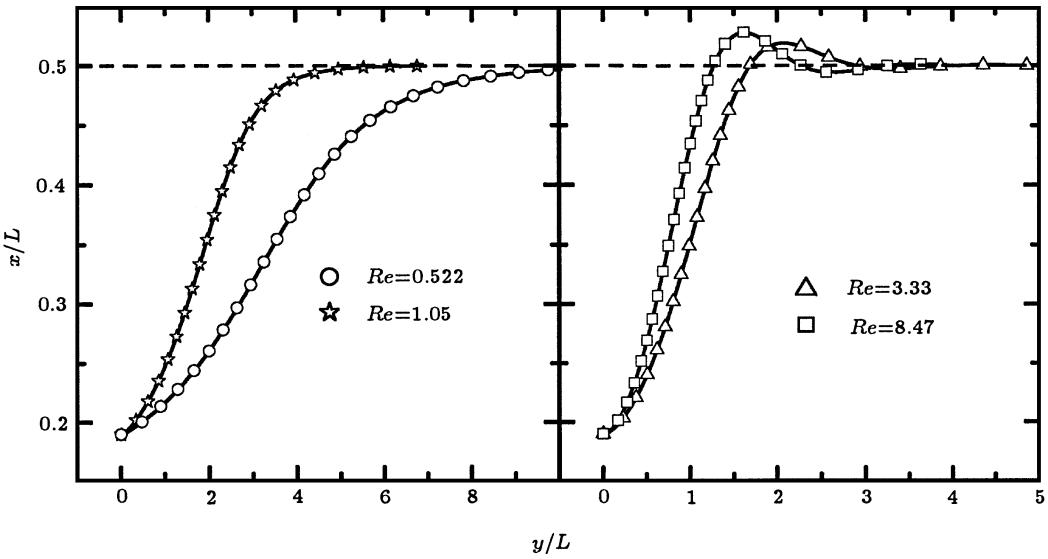
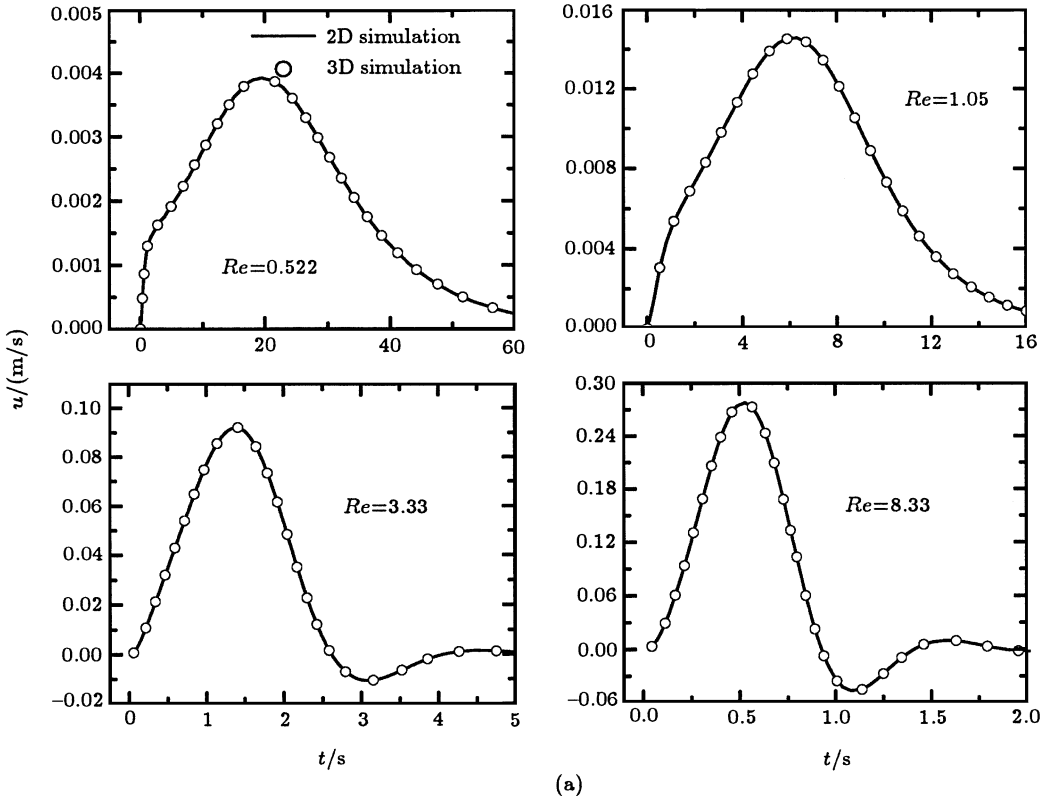
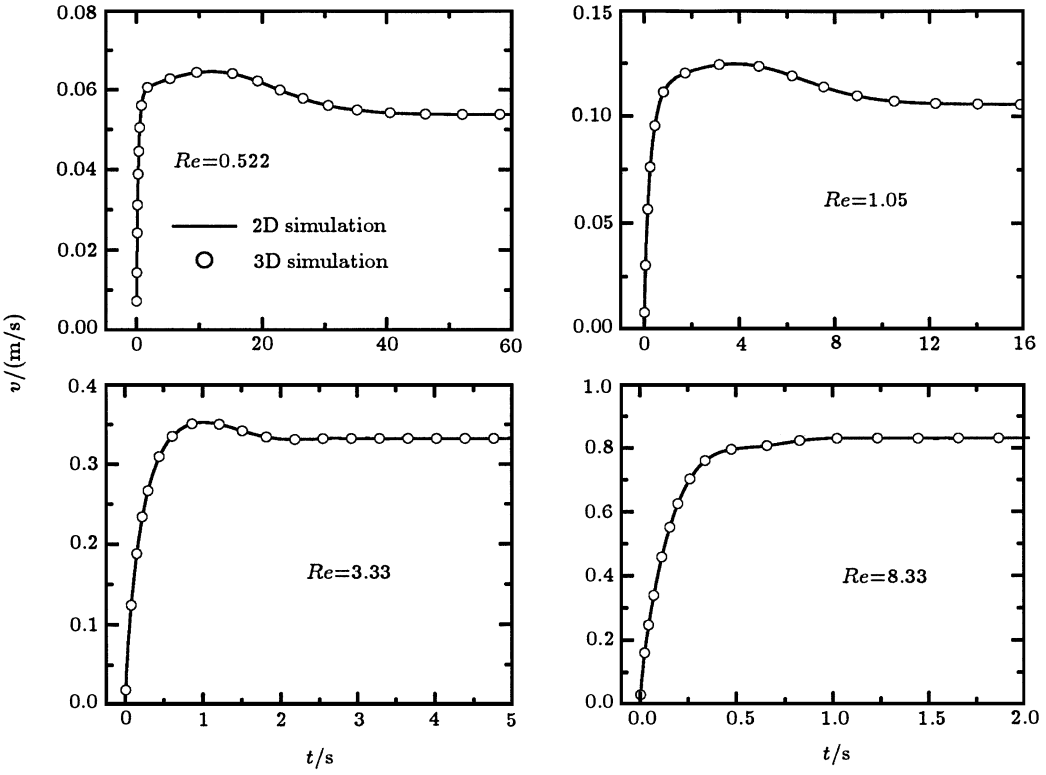


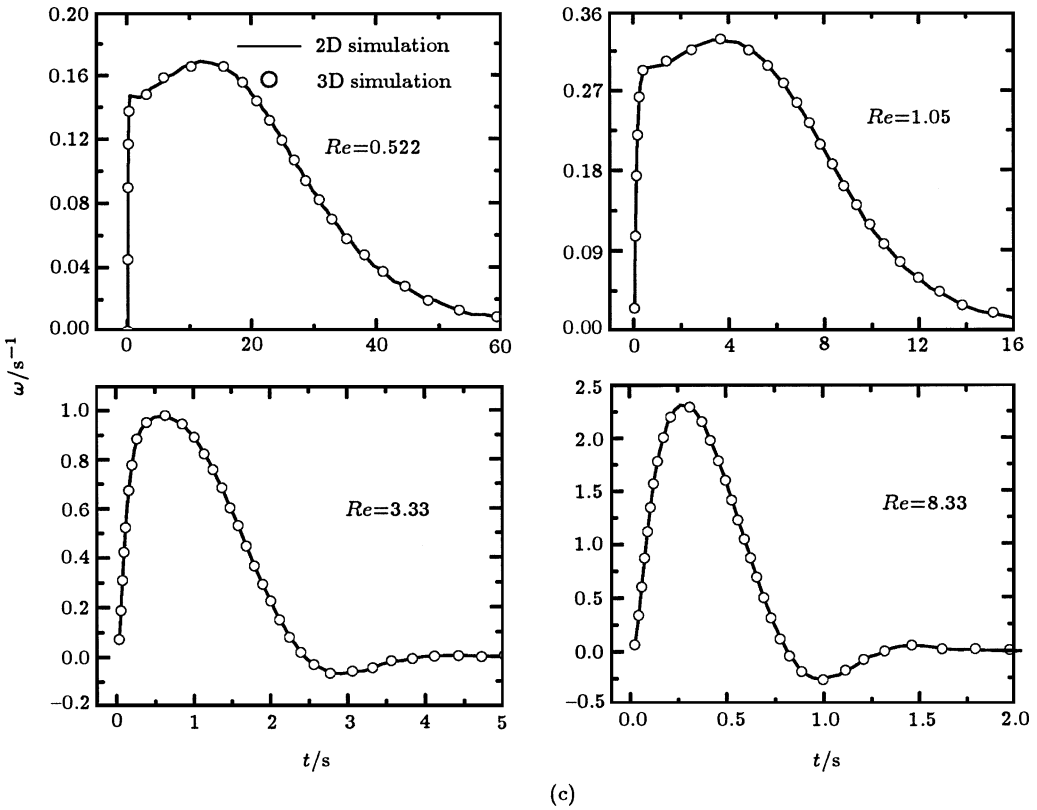
Fig.3. The trajectories of a circular particle settled in a 2D vertical tube from an off-centre initial position at different terminal Reynolds. The lines and symbols are obtained from the 2D and 3D lattice Boltzmann simulations, respectively.



(a)



(b)



(c)

Fig.4. Horizontal velocity (u), vertical velocity (v) and angular velocity (ω) of a circular particle settled in a 2D vertical tube from an off-centre initial position at different terminal Reynolds. The lines and symbols are obtained from 2D and 3D lattice Boltzmann simulations, respectively.

6. Conclusion

We have extended the 2D lattice Boltzmann method on moving particles in a Newtonian fluid to 3D cases. The simulation results on a single sphere in a square tube at very low Reynolds numbers agree with experimental data to a high accuracy. The time-dependent behaviour of a circular cylinder in a 2D channel obtained from simulations is consistent with the previous 2D scheme. These results demonstrate the accuracy and efficiency of the proposed 3D scheme. We emphasize that highly accurate simulation results can be achieved with fewer meshes compared with the previous lattice Boltzmann methods, since much exact spatial location of the physical boundary of the suspended particles can be determined in the present scheme. The present scheme is expected to find applications to the flow system with moving boundaries, such as the blood flow in distensible vessels, the particle–flow interaction and the solidification.

References

[1] McNamara G R and Zanetti G 1988 *Phys. Rev. Lett.* **61** 2332

[2] Chen S, Chen H, Martinez D O and Matthaeus W H 1991 *Phys. Rev. Lett.* **67** 3776

[3] Qian Y H, d'Humiéres D and Lallemand P 1992 *Europhys. Lett.* **17** 479

[4] Chen S Y and Doolen G D 1998 *Annu. Rev. Fluid Mech.* **30** 329

[5] Ladd A J C 1994 *J. Fluid Mech.* **271** 285

[6] Aidun C K, Lu Y and Ding E 1998 *J. Fluid Mech.* **373** 287

[7] Behrend O 1995 *Phys. Rev.* E **52** 1164

[8] Raiskinmaki P *et al* 2000 *Comput. Phys. Commun.* **129** 185

[9] Noble D R and Torczynski J R 1998 *Int. J. Mod. Phys.* C **9** 1189

[10] Fang H P, Lin Z F and Wang Z W 1998 *Phys. Rev.* E **57** R25

[11] Fang H P, Wang Z W, Lin Z F and Liu M R 2002 *Phys. Rev.* E **65** 51905

[12] Inamuro T, Maeba K and Ogino F 2000 *Int. J. Multiphase Flow* **26** 1981

[13] Filippova O and Hanel D 1997 *Comput. Fluids* **26** 697

[14] Mei R, Lou L and Shyy W 1999 *J. Comput. Phys.* **155** 307

[15] Mei R, Shyy W, Yu D and Lou L 2000 *J. Comput. Phys.* **161** 680

[16] Fang H P, Noble D R, Hu H H and Chen S Y *J. Comput. Phys.* to be published

[17] Hu H H, Joseph D D and Crochet M J 1992 *Theor. Comput. Fluid Dyn.* **3** 285

[18] Feng J, Hu H H and Joseph D D 1994 *J. Fluid Mech.* **261** 95

[19] Allen M P and Tildesley D J 1987 *Computer Simulation of Liquid* (Oxford: Clarendon)

[20] Miyamura A, Iwasaki S and Ishii T 1981 *Int. J. Multiphase Flow* **7** 41